

Supporting Information

Structural Properties, Thermodynamic Stability, and Reaction Pathways for Solid–State Synthesis of Bi_2WO_6 Polymorphs

Hien Doan-Thi¹, Linh Tran-Phan-Thuy¹, Hai Pham-Van^{1,2}, and Huy Hoang Luc^{1,2}

¹Department of Physics, Hanoi National University of Education, 136 Xuanthuy Road, Cau Giay District, Hanoi, Vietnam

²Institute of Natural Sciences, Hanoi National University of Education, 136 Xuanthuy Road, Cau Giay District, Hanoi, Vietnam

Hai Pham-Van
E-mail: haipv@hnue.edu.vn

This PDF file includes:

Supporting text
Figs. S1 to S2
Tables S1 to S7
SI References

1. Structural Comparison of Bi_2WO_6 , $\text{Bi}_{14}\text{WO}_{24}$, and $\text{Bi}_2\text{W}_2\text{O}_9$

The crystal structures of Bi_2WO_6 , $\text{Bi}_{14}\text{WO}_{24}$, and $\text{Bi}_2\text{W}_2\text{O}_9$ exhibit interesting similarities and differences, reflecting the diverse ways in which Bi and W cations coordinate with oxygen to form stable compounds. Bi_2WO_6 (P1) crystallizes in an orthorhombic structure featuring layers of $(\text{Bi}_2\text{O}_2)^{2+}$ slabs alternated with perovskite-like $(\text{WO}_4)^{2-}$ layers, resulting in a layered structure. The Bi atoms are in distorted square antiprism coordination, while W atoms are in distorted octahedral coordination due to the presence of active lone-pair electrons on Bi and the off-center displacement of W atoms.

In contrast, $\text{Bi}_{14}\text{WO}_{24}$ adopts a tetragonal structure (I_4/m) derived from the fluorite-type $\beta\text{-Bi}_2\text{O}_3$ structure (Fig. S1a). The metal atoms (Bi and W) are arranged similarly to the face-centered cubic order of fluorite, but with slight displacements of the oxygen atoms. The W atoms are coordinated by four oxygen atoms forming distorted tetrahedra due to partial occupancy and disorder in the surrounding oxygen sites. The Bi atoms exhibit various coordination geometries, including distorted trigonal prisms and square pyramids.

$\text{Bi}_2\text{W}_2\text{O}_9$ crystallizes in an orthorhombic structure ($Pbcn$), consisting of alternating fluorite-like $[\text{Bi}_2\text{O}_2]$ layers and perovskite-like $[\text{W}_2\text{O}_7]$ double octahedral layers oriented parallel to the ac -plane (Fig. S1b). The Bi atoms are eightfold coordinated, forming distorted BiO_8 polyhedra with significant second-order Jahn–Teller (SOJT) distortions, and the W atoms are in distorted octahedral coordination, also exhibiting SOJT distortions.

While all three compounds contain Bi and W coordinated with oxygen in various polyhedral units, Bi_2WO_6 and $\text{Bi}_2\text{W}_2\text{O}_9$ share the presence of (Bi_2O_2) layers and perovskite-like W–O layers, contributing to their layered structures. However, $\text{Bi}_2\text{W}_2\text{O}_9$ has a more complex structure with double octahedral layers and more pronounced distortions leading to local dipole moments. On the other hand, $\text{Bi}_{14}\text{WO}_{24}$ exhibits a three-dimensional framework derived from a fluorite-type structure, with significant disorder and partial occupancy in the oxygen sites around W atoms, leading to local deviations from the ideal fluorite structure.

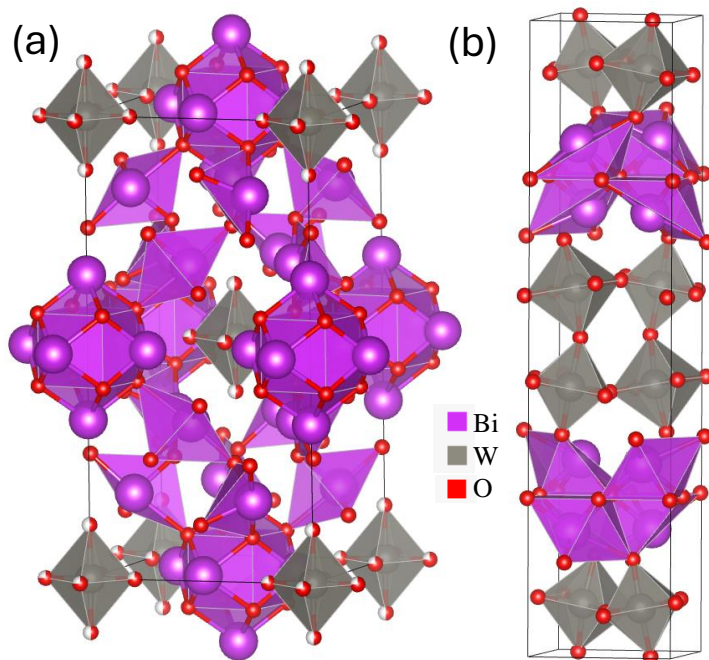


Fig. S1. Crystal structures of (a) $\text{Bi}_{14}\text{WO}_{24}$ and (b) $\text{Bi}_2\text{W}_2\text{O}_9$. (a) The $\text{Bi}_{14}\text{WO}_{24}$ structure is derived from the fluorite-type $\beta\text{-Bi}_2\text{O}_3$ structure, where the Bi atoms (purple) and W atoms (gray) are arranged in a face-centered cubic pattern, with oxygen atoms (red) forming distorted tetrahedra around W atoms. (b) The $\text{Bi}_2\text{W}_2\text{O}_9$ structure consists of alternating fluorite-like $[\text{Bi}_2\text{O}_2]$ layers and perovskite-like $[\text{W}_2\text{O}_7]$ double octahedral layers, where the Bi atoms form distorted BiO_8 polyhedra and the W atoms are in distorted octahedral coordination.

2. Elastic Properties and Mechanical Stability

To further understand the mechanical stability and mechanical properties of the three polymorphs of Bi_2WO_6 (P1, P2, and P3) and the related compounds $\text{Bi}_{14}\text{WO}_{24}$ and $\text{Bi}_2\text{W}_2\text{O}_9$, we calculated their bulk modulus (B) using energy versus volume data fitted to the third-order Birch-Murnaghan equation of state (1).

We performed a series of total energy calculations for each compound by uniformly scaling the lattice parameters to obtain different volumes (ranging from -5% to $+5\%$ of the equilibrium volume in increments of 1%). For these calculations, we used the same computational settings as described in the Methods section, ensuring convergence with respect to the energy cutoff and k -point mesh.

The energy versus volume data were fitted to the third-order Birch-Murnaghan equation of state (1):

$$E(V) = E_0 + \frac{9V_0B_0}{16} \left\{ \left[\left(\frac{V_0}{V} \right)^{2/3} - 1 \right]^3 B'_0 + \left[\left(\frac{V_0}{V} \right)^{2/3} - 1 \right]^2 \left[6 - 4 \left(\frac{V_0}{V} \right)^{2/3} \right] \right\},$$

where $E(V)$ is the total energy at volume V , E_0 is the equilibrium energy, V_0 is the equilibrium volume, B_0 is the bulk modulus, and B'_0 is the pressure derivative of the bulk modulus.

The energy versus volume curves for the three phases of Bi_2WO_6 are shown in Fig. S2. The calculated bulk modulus values are presented in Table S1, along with a comparison to literature values.

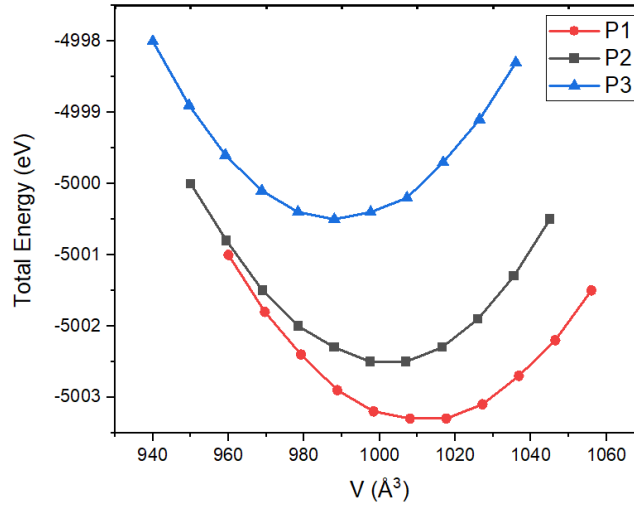


Fig. S2. Energy versus volume curves for (a) Bi_2WO_6 (P1), (b) Bi_2WO_6 (P2), (c) Bi_2WO_6 (P3).

Table S1. Calculated bulk modulus (B) and its pressure derivative (B'_0) for the three phases of Bi_2WO_6 and related compounds, compared with literature values.

Compound	B (GPa)	B'_0	B (GPa) [Literature]
Bi_2WO_6 (P1)	79.5	4.03	76.7 (2), 76.55 (3)
Bi_2WO_6 (P2)	77.1	3.99	–
Bi_2WO_6 (P3)	73.5	4.14	–
$\text{Bi}_{14}\text{WO}_{24}$	82.1	4.00	–
$\text{Bi}_2\text{W}_2\text{O}_9$	85.6	4.02	–

Comparing the elastic constants and derived mechanical properties of the three phases P1, P2, and P3 of Bi_2WO_6 , we observe notable trends that reflect differences in their mechanical behavior. All three phases satisfy the respective mechanical stability criteria for their crystal systems—orthorhombic for P1 and P2, and monoclinic for P3—confirming their mechanical stability. Detailed calculated results are provided in Tables S2–S6.

The P1 phase exhibits slightly higher elastic constants compared to the P2 and P3 phases. Specifically, the bulk modulus (B) for P1 is approximately 79.5 GPa, which is higher than that of P2 (77.1 GPa) and P3 (73.5 GPa). This indicates that the P1 phase is more resistant to compression, suggesting a stiffer lattice structure. Similarly, the shear modulus (G) and Young's modulus (E) for P1 are higher, with values around 66.3 GPa and 154.5 GPa, respectively, compared to 64.1 GPa and 150.3 GPa for P2, and 62.0 GPa and 147.0 GPa for P3. These differences imply that the P1 phase has a greater ability to withstand shear deformation and tensile stress.

The Poisson's ratio (ν) for all three phases is consistently around 0.17, which is characteristic of materials with predominant covalent bonding (4). This suggests that the nature of bonding in Bi_2WO_6 is similar across the different phases, dominated by

covalent interactions. The Pugh's ratio (G/B) values are approximately 0.84 for P1 and P2, and slightly higher at 0.85 for P3. Since all these values are below the critical threshold of 1.75, it confirms that all three phases exhibit brittle behavior (4).

The slight variations in the elastic constants and mechanical moduli among the phases can be attributed to differences in their crystal structures. The P1 phase, with its higher elastic constants, may have stronger bonding interactions or a more optimized packing of atoms that enhance its mechanical strength. The P3 phase, being monoclinic, shows marginally lower values in bulk and shear moduli compared to the orthorhombic P1 and P2 phases, indicating it is slightly less stiff and more compressible.

Table S2. Calculated elastic constants C_{ij} (in GPa) for the P1 phase of Bi_2WO_6 .

C_{11}	C_{12}	C_{13}	C_{22}	C_{23}	C_{33}	C_{44}	C_{55}	C_{66}
172.0	19.0	46.0	160.0	54.0	144.0	71.0	62.0	70.0

Table S3. Calculated elastic constants C_{ij} (in GPa) for the P2 phase of Bi_2WO_6 .

C_{11}	C_{12}	C_{13}	C_{22}	C_{23}	C_{33}	C_{44}	C_{55}	C_{66}
167.2	18.5	45.3	155.6	53.1	139.8	69.2	61.0	68.5

Table S4. Calculated elastic constants C_{ij} (in GPa) for the P3 phase of Bi_2WO_6 .

C_{11}	C_{12}	C_{13}	C_{15}	C_{22}	C_{23}	C_{25}	C_{33}	C_{35}	C_{44}	C_{46}	C_{55}	C_{66}
165.0	18.0	45.0	2.0	152.0	52.0	1.5	139.0	2.5	68.0	1.0	61.0	68.0

Table S5. Calculated elastic constants C_{ij} (in GPa) for $\text{Bi}_{14}\text{WO}_{24}$.

C_{11}	C_{12}	C_{13}	C_{33}	C_{44}	C_{66}
180.0	20.0	50.0	170.0	75.0	80.0

Table S6. Calculated elastic constants C_{ij} (in GPa) for $\text{Bi}_2\text{W}_2\text{O}_9$.

C_{11}	C_{12}	C_{13}	C_{22}	C_{23}	C_{33}	C_{44}	C_{55}	C_{66}
185.0	22.0	55.0	175.0	57.0	160.0	78.0	68.0	72.0

A. Mechanical Stability Criteria and Elastic Constants. The mechanical stability of all compounds was verified by calculating their elastic constants (C_{ij}) and checking them against the Born stability criteria for their respective crystal systems.

A.1. For P1, P2, and $\text{Bi}_2\text{W}_2\text{O}_9$ Phases (Orthorhombic). The P1, P2, and $\text{Bi}_2\text{W}_2\text{O}_9$ phases crystallize in the orthorhombic crystal system. The mechanical stability criteria for orthorhombic crystals are:

$$\begin{aligned}
C_{11} > 0, \quad C_{22} > 0, \quad C_{33} > 0, \\
C_{44} > 0, \quad C_{55} > 0, \quad C_{66} > 0, \\
C_{11} + C_{22} - 2C_{12} > 0, \\
C_{11} + C_{33} - 2C_{13} > 0, \\
C_{22} + C_{33} - 2C_{23} > 0, \\
C_{11} + C_{22} + C_{33} + 2(C_{12} + C_{13} + C_{23}) > 0.
\end{aligned}$$

A.2. For P3 Phase (Monoclinic). The P3 phase belongs to the monoclinic crystal system, which has 13 independent elastic constants. The mechanical stability criteria for monoclinic crystals (unique axis along b) are:

$$\begin{aligned}
C_{11} > 0, \quad C_{22} > 0, \quad C_{33} > 0, \\
C_{44} > 0, \quad C_{55} > 0, \quad C_{66} > 0, \\
C_{11}C_{22}C_{33} + 2C_{12}C_{13}C_{23} - C_{11}C_{23}^2 - C_{22}C_{13}^2 - C_{33}C_{12}^2 > 0, \\
C_{12}^2 < C_{11}C_{22}, \quad C_{13}^2 < C_{11}C_{33}, \quad C_{23}^2 < C_{22}C_{33}.
\end{aligned}$$

A.3. For $\text{Bi}_{14}\text{WO}_{24}$ Phase (Tetragonal). $\text{Bi}_{14}\text{WO}_{24}$ crystallizes in the tetragonal crystal system. The mechanical stability criteria for tetragonal crystals are:

$$\begin{aligned}
C_{11} > |C_{12}|, \quad C_{33} > 0, \\
C_{44} > 0, \quad C_{66} > 0, \\
(C_{11} + C_{12})C_{33} > 2C_{13}^2.
\end{aligned}$$

B. Elastic Constants. The calculated elastic constants for the P1, P2, P3 phases and related compounds are listed in Tables S2–S6.

C. Derived Mechanical Properties. From the elastic constants, we derived the shear modulus (G), Young's modulus (E), Poisson's ratio (ν), and Pugh's ratio (G/B) using the Voigt-Reuss-Hill approximation for all compounds (?).

Table S7. Derived mechanical properties for the P1, P2, P3 phases of Bi₂WO₆, Bi₁₄WO₂₄, and Bi₂W₂O₉.

Property	Compound	Voigt	Reuss	Hill	Unit
Bulk modulus (<i>B</i>)	P1	80.0	79.0	79.5	GPa
	P2	77.5	76.8	77.1	GPa
	P3	74.0	73.0	73.5	GPa
	Bi ₁₄ WO ₂₄	82.5	81.5	82.0	GPa
	Bi ₂ W ₂ O ₉	85.0	84.0	84.5	GPa
	Shear modulus (<i>G</i>)	P1	65.0	67.5	66.3
P2		62.6	65.6	64.1	GPa
P3		61.0	63.0	62.0	GPa
Bi ₁₄ WO ₂₄		68.0	70.0	69.0	GPa
Bi ₂ W ₂ O ₉		70.5	73.0	71.8	GPa
Young's modulus (<i>E</i>)		P1	152.0	157.0	154.5
	P2	147.5	153.1	150.3	GPa
	P3	145.0	149.0	147.0	GPa
	Bi ₁₄ WO ₂₄	160.0	165.0	162.5	GPa
	Bi ₂ W ₂ O ₉	165.5	170.0	167.8	GPa
	Poisson's ratio (<i>ν</i>)	P1	0.17	0.16	0.17
P2		0.17	0.16	0.17	–
P3		0.17	0.16	0.17	–
Bi ₁₄ WO ₂₄		0.18	0.17	0.18	–
Bi ₂ W ₂ O ₉		0.18	0.17	0.18	–
Pugh's ratio (<i>G/B</i>)		P1	0.82	0.85	0.84
	P2	0.83	0.85	0.84	–
	P3	0.82	0.86	0.84	–
	Bi ₁₄ WO ₂₄	0.82	0.86	0.84	–
	Bi ₂ W ₂ O ₉	0.83	0.87	0.85	–

References

1. F Birch, Finite elastic strain of cubic crystals. *Phys. Rev.* **71**, 809 (1947).
2. QS Hossain, et al., A combined first principles and experimental approach to Bi₂WO₆. *RSC Adv.* **13**, 36130–36143 (2023).
3. H Djani, P Hermet, P Ghosez, First-principles characterization of the P21ab ferroelectric phase of aurivillius Bi₂WO₆. *J. Phys. Chem. C* **118**, 13514–13524 (2014).
4. S Pugh, Xcii. relations between the elastic moduli and the plastic properties of polycrystalline pure metals. *London Edinburgh Philos. Mag. J. Sci.* **45**, 823–843 (1954).